[Mn(4)(III)Ln(4)(III)] Calix[4]arene Clusters as Enhanced Magnetic Coolers and Molecular Magnets

Cite as:
Karotsis, G., Kennedy, S., Teat, S. J., Beavers, C. M., Fowler, D. A., Morales, J. J., Evangelisti, M., Dalgarno, S. J., & Brechin, E. K. (2010). [$Mn^{III}_4Ln^{III}_4$] Calix[4]arene Clusters as Enhanced Magnetic Coolers and Molecular Magnets. *Journal of the American Chemical Society*, 132(37), 12983-12990.

Manuscript received: 15/06/2010; Accepted: 02/08/2010; Article published: 22/09/2010

[$Mn^{III}_4Ln^{III}_4$] Calix[4]arene Clusters as Enhanced Magnetic Coolers and Molecular Magnets**

Georgios Karotsis,[1] Stuart Kennedy,[2] Simon J. Teat,[3] Christine M. Beavers,[3] Drew A. Fowler,[4] Juan J. Morales,[5] Marco Evangelisti, [6,]* Scott J. Dalgarno,[2,]* Euan K. Brechin[1,]*

[1]EaStCHEM, School of Chemistry, Joseph Black Building, University of Edinburgh, West Mains Road, Edinburgh, EH9 3JJ, UK.

[2]School of Engineering and Physical Sciences – Chemistry, Heriot-Watt University, Riccarton, Edinburgh, EH14 4AS, Scotland, UK.

[3]Advanced Light Source, Berkeley Laboratory, 1 Cyclotron Road, MS6R2100, Berkeley, CA 94720, USA.

[4]Department of Chemistry, University of Missouri, 601 S. College Ave., Columbia, MO 65211, USA.

[5]Departamento de Física de la Materia Condensada, Universidad de Zaragoza, 50009 Zaragoza, Spain.

[6]Instituto de Ciencia de Materiales de Aragón, CSIC-Universidad de Zaragoza, Departamento de Física de la Materia Condensada, 50009 Zaragoza, Spain.

[*]Corresponding authors; M.E. e-mail: evange@unizar.es; S.J.D. e-mail: S.J.Dalgarno@hw.ac.uk; E.K.B. e-mail: ebrechin@staffmail.ed.ac.uk

[**]EKB and SJD thank the EPSRC and Leverhulme Trust for funding and Heriot-Watt University for a studentship (SK). ME thanks the Spanish Ministry for Science and Innovation for grants MAT2009-13977-C03 and CSD2007-00010. The Advanced Light Source is supported by the Director, Office of Science, Office of Basic Energy Sciences, of the US Department of Energy under contract no. DE-AC02-05CH11231.

Supporting information:
Temperature dependence of the out-of-phase ac-susceptibility and crystallographic data (CIF) for 2 and 3. This material is available free of charge via the Internet at http://pubs.acs.org

Graphical abstract

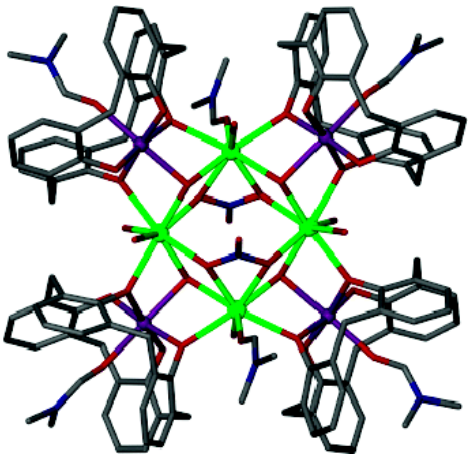

Synopsis

Calix[4]arene based $[Mn^{III}_4Ln^{III}_4]$ clusters (Ln = Gd, Tb, Dy) act as molecular coolers *or* molecular magnets depending on the isotropy of the lanthanide ion employed in cluster formation.

Keywords

structural coordination chemistry; transition-metal; low-temperature; ground-state; Fe-III; complexes; refrigeration; calixarenes; capsules; alcohols

Abstract

The use of methylene-bridged calix[4]arenes in 3*d*/4*f* chemistry produces a family of clusters of general formula $[Mn^{III}_4Ln^{III}_4(OH)_4(C4)_4(NO_3)_2(DMF)_6(H_2O)_6](OH)_2$ (where C4 is calix[4]arene; Ln = Gd (**1**), Tb (**2**), Dy (**3**)). The molecular structure describes and square of Ln^{III} ions housed within a square of Mn^{III} ions. Magnetic studies reveal that **1** has a large number of molecular spin states that are populated even at the lowest investigated temperatures, whilst the ferromagnetic limit $S = 22$ is being approached only at the highest applied fields. This, combined with the high magnetic isotropy, enables the complex to be an excellent magnetic refrigerant for low-temperature applications. Replacement of the isotropic Gd^{III} ions with the anisotropic Tb^{III} and Dy^{III} ions "switches" the magnetic properties of the cluster so that they (**2** and **3**) behave as low-temperature molecular magnets displaying slow relaxation of the magnetisation.

Introduction

Magnetic refrigeration constitutes one of the potential applications envisioned for polymetallic molecules.[1] The Magneto-Caloric Effect (MCE) is based on the change of magnetic entropy upon application of a magnetic field and is of great technological importance since it can be used for cooling applications according to a process known as adiabatic demagnetisation.[2,3] This energy-efficient and environmentally friendly technique is particularly promising for refrigeration in the ultra-low-temperature region, providing for example a valid alternative to the use of ^{3}He which is becoming rare and expensive.[4] Recent studies have demonstrated that the MCE of selected molecular cluster compounds can be much larger than in the best, and conventionally studied, inter-metallic and lanthanide alloys, and magnetic nanoparticles. The recipe[5] required for making such molecules requires them to have a negligible anisotropy which therefore permits easy polarization of the net molecular spin, leading to a large magnetic entropy change and the presence of degenerate or low-lying excited spin states, since the so-added degrees of freedom result in extra magnetic entropy. In short, we must target high spin (ferromagnetic) isotropic clusters displaying weak intra-molecular magnetic exchange. The [Mn_{12}] and [Fe_8] molecular magnets were the first to be investigated for magnetic refrigeration because of their well-defined $S = 10$ ground states, and although they displayed relatively large $-\Delta S_m$ values the large anisotropy present in both systems freezes the orientation of the molecular spins once the temperature is lowered below ~ 4K, limiting their applicability.[1,6,7] The first isotropic molecular cluster studied was the heterometallic [Cr_7Cd] wheel,[8] but the problem in this case was the low value of the spin, $S = 3/2$. A huge step forward in the search for truly applicable molecular candidates was accomplished via the synthesis and study of highly-symmetric molecules with large values of the spin ground state. The first was [Fe_{14}] with an $S = 25$ ground state,[9] the second a ferromagnetic [Mn_{10}] supertetrahedron with $S = 22$ displaying practically zero anisotropy,[10] and the third a [Mn_{14}] disc[11] displaying a truly enormous enhancement of the MCE with values of $-\Delta S_m$ as large as 20 $Jkg^{-1}K^{-1}$ for liquid-helium temperatures and $\Delta B = 6$ T - almost a factor of two larger than that of [$DyCo_2$] nanoparticles.[12] One of our long-standing synthetic strategies for making high spin molecular clusters is the use of polyalkoxide ligands such as the tripodal 1,1,1-tris(hydroxymethyl)ethane, 1,1,1-tris(hydroxymethyl)propane and pentaerythritol.[13] The disposition of the three alkoxide arms of the tri-anions of $RC(CH_2OH)_3$ pro-ligands direct the formation of triangular [M_3] units where each arm of the ligand bridges one edge of the triangle. These triangular building blocks then self-assemble to form elaborate architectures (M_9 partial icosahedra,[14] M_{10} supertetrahdra,[10] Mn_{32} truncated cubes[15] *etc*) whose topologies are dependent on reaction conditions and/or the presence of other bridging and/or terminal co-ligands such as carboxylates or β–diketonates *etc*.[13] A natural extension of this strategy is the use of tetrapodal alkoxides such as calix[4]arenes. Calix[4]arenes are cyclic molecules that have been used extensively in the formation of supramolecular structures and in various fields of coordination chemistry.[16] Calix[4]arene (C4, Figure

1A) is a cyclic polyphenol that is synthetically accessible on a large scale via the parent *p*-^{t}Bu derivative (TBC4),[17] and this molecule is the typical starting point for synthetic alteration to the general molecular framework.[18] In a bowl-conformation, the calix[4]arene polyphenolic pocket at the lower-rim is an attractive feature for metal complexation.[19] We,[20] and others,[21] have been using methylene bridged calix[4]arenes for the construction of polynuclear metal clusters possessing interesting magnetic properties. In addition, thia- and sulfonyl-bridged calix[4]arenes have also been used in this regard, but these molecules form distinctly different cluster motifs due to the bridging atoms taking part in the coordination chemistry of the resulting complexes.[22] With methylene bridged TBC4, we have recently synthesised and characterised [$Mn^{III}_2Mn^{II}_2$] Single-Molecule Magnets (SMMs, Figure 1B),[20a] enneanuclear Cu^{II} tri-capped trigonal prismatic clusters that act as versatile anion binding materials (Figure 1C)[20b] and a [$Mn^{III}_4Gd^{III}_4$] cluster that displays an enhanced MCE.[20c] This paper extends our original communication on the latter and describes the syntheses, structures and magnetic properties of a family of [$Mn^{III}_4Ln^{III}_4$] clusters, the first methylene bridged calix[*n*]arene based 3*d*-4*f* molecules, in which the replacement of one Ln(III) ion for another invokes dramatic changes in the observed magnetic properties in otherwise structurally analogous molecules.

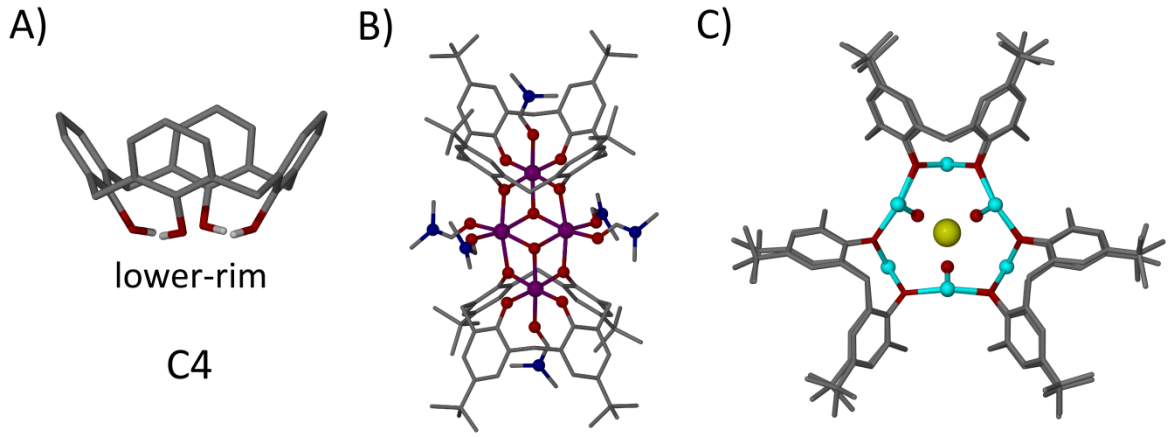

Figure 1. A) Calix[4]arene, C4. B) The [$Mn^{III}_2Mn^{II}_2$] SMM formed with TBC4.[20a] C) View down the centre of a tri-capped trigonal prismatic enneanuclear Cu^{II} cluster formed with TBC4, and that binds two chloride anions (one above and below the cluster core).[20b] Figures not to scale. Hydrogen atoms omitted for clarity in A – C (except for lower-rim hydroxyl groups in A). Ligated solvent molecules and solvent of co-crystallization omitted for clarity in C. Colour code, Mn = purple; O = red; N = dark blue; C = grey; Cu = light blue; Cl = yellow.

Experimental details

$Mn(NO_3)_2{\cdot}4H_2O$ (0.1 g, 0.39 mmol), $Gd(NO_3)_2{\cdot}6H_2O$ (0.1 g, 0.22 mmol) and C4 (0.1 g, 0.23 mmol) were dissolved in a mixture of DMF (10 cm^3) and MeOH (10 cm^3). Following 5 minutes of stirring, NEt_3 (0.2 g, 1.97 mmol) was added dropwise, and the resulting purple solution was stirred for a further hour. X-ray quality crystals were obtained in good yield (40%) after slow evaporation of the mother liquor. Elemental analysis (%) calculated for (**1**), $C_{130}H_{140}Mn_4Gd_4N_8O_{40}$: C 47.27, H 4.27, N 3.39; Found: C 47.02, H 4.14, N 3.27.

Complexes **2** and **3** were made in an analogous manner using $Tb(NO_3)_3{\cdot}6H_2O$ and $Dy(NO_3)_3{\cdot}6H_2O$ in place of $Gd(NO_3)_3{\cdot}6H_2O$. Elemental analysis (%) calculated for (**2**), $C_{135}H_{155}Mn_4Tb_4N_9O_{43}$: C 47.04, H 4.53, N 3.66; Found: C 46.98, H 4.24, N 3.59. Elemental analysis (%) calculated for (**3**), $C_{130}H_{140}Mn_4Dy_4N_8O_{40}$: C 46.97, H 4.24, N 3.37; Found: C 46.51, H 4.18, N 3.25.

General crystallographic details

Data for **1**[20c] and **2** were collected on a Bruker Nonius X8 Apex II diffractometer operating with MoKα radiation (λ = 0.71073 Å) at T = 100(2) K. Data for **3** were collected on a Bruker Apex II CCD diffractometer operating with synchrotron radiation (λ = 0.77490 Å) at T = 100(2) K. The routine SQUEEZE was applied to the data for **1** – **3** due to the presence of badly disordered solvent molecules.[23] In all cases, this had the effect of dramatically improving the agreement indices. **Crystal data for 1:**[20c] $C_{130}H_{122}Gd_4Mn_4N_8O_{42}$, M = 3317.12, Black Block, 0.25 × 0.20 × 0.18 mm^3, monoclinic, space group $C2/c$ (No. 15), a = 34.41(3), b = 12.397(9), c = 32.15(4) Å, β = 98.14(3)°, V = 13576(22) $Å^3$, Z = 4, $2\theta_{max}$ = 46.8º, 56018 reflections collected, 9621 unique (R_{int} = 0.0831). Final *GooF* = 1.015, *R1* = 0.0462, *wR2* = 0.1217, *R* indices based on 7169 reflections with I >2sigma(I) (refinement on F^2). **Crystal data for 2:** $C_{135}H_{155}Mn_4N_9O_{43}Tb_4$, M = 3447.12, Black Block, 0.40 × 0.32 × 0.28 mm^3, triclinic, space group P-1 (No. 2), a = 17.87(5), b = 19.62(5), c = 23.80(7) Å, α = 102.46(4), β = 104.83(4), γ = 96.28(4)°, V = 7754(37) $Å^3$, Z = 2, $2\theta_{max}$ = 46.5º, 143013 reflections collected, 21725 unique (R_{int} = 0.0857). Final *GooF* = 0.977, *R1* = 0.0507, *wR2* = 0.1290, *R* indices based on 14442 reflections with I >2sigma(I) (refinement on F^2). **Crystal data for 3**: $C_{130}H_{140}Dy_4Mn_4N_8O_{40}$, M = 3324.26, Purple Plate, 0.20 × 0.06 × 0.02 mm^3, triclinic, space group P-1 (No. 2), a = 17.805(2), b = 19.781(2), c = 23.563(3) Å, α = 102.752(2), β = 104.586(2), γ = 96.203(2)°, V = 7714.9(15) $Å^3$, Z = 2, D_c = 1.431 g/cm^3, F_{000} = 3320, Bruker Apex II CCD Diffractometer, synchrotron radiation, λ = 0.77490 Å, T = 100(2)K, $2\theta_{max}$ = 51.1º, 64375 reflections collected, 22184 unique (R_{int} = 0.0609). Final *GooF* = 0.921, *R1* = 0.0511, *wR2* = 0.1219, *R* indices based on 15071 reflections with I

>2sigma(I) (refinement on F^2), 1764 parameters, 147 restraints. Lp and absorption corrections applied, μ = 2.877 mm^{-1}.

Magnetic Data and Analysis

Magnetisation measurements down to 2 K and specific heat measurements using the relaxation method down to 0.3 K on powdered crystalline samples of (**1**)-(**3**) were carried out by means of commercial setups for the (0 – 9) T magnetic field range. Ac-susceptibility measurements were extended down to 80 mK with a homemade susceptometer, installed in a dilution refrigerator.

Results and Discussion

The reaction of $Mn(NO_3)_2{\cdot}4H_2O$ and $Ln(NO_3)_3{\cdot}6H_2O$ with C4 and NEt_3 in a solvent cocktail of MeOH/DMF results in the formation of complexes with the general formula $[Mn^{III}_4Ln^{III}_4(OH)_4(C4)_4(NO_3)_2(DMF)_6(H_2O)_6](OH)_2$, where Ln = Gd (**1**), Tb(**2**), or Dy (**3**). Crystals of **1** are in the monoclinic space group *C*2/*c*, whilst those of **2** and **3** are found to crystallise in the triclinic space group *P*-1. The C4 supported clusters in all three complexes are structurally analogous, differing only in the number of co-crystallised solvent molecules (which are badly disordered), and so for the sake of brevity we will limit our discussion to complex **1**, highlighting any specific differences between the molecules at appropriate stages. The cluster (Figure 2) comprises a near-planar octametallic core describing a "square" of Mn(III) ions encasing a "square" of Gd(III) ions. The $\{Mn_4\}$ square has dimensions 6.591 x 7.042 Å and the $\{Gd_4\}$ square 3.915 x 3.929 Å, with the latter rotated approximately 45° with respect to the former. This is a very unusual motif, but has also been observed recently in the cluster $[Mn_4Nd_4(OH)_4(fcdc)_2(Piv)_8(bdea)_4]{\cdot}H_2O$ (fcdc = ferrocene dicarboxylate; piv = pivalate or trimethyacetate; $bdeaH_2$ = *N*-butyldiethanolamine).[24] The central $[Gd^{III}_4(OH)_4(NO_3)_2]$ unit comprises the four Gd(III) ions connected to each other via four μ_3-OH^- ions (O12 and O16 and symmetry equivalents) and two η^2, η^2, μ_3-NO_3^- ions. The OH^- ions also bridge to the four $[Mn^{III}(C4)(DMF)]$ corner units of the $\{Mn_4\}$ square. The μ_3-TBC4 ligands are fully deprotonated with two oxygen atoms (O1, O4 and O7, O8 and symmetry equivalents) bonding terminally to the Mn(III) ions and two (O2, O3 and O6, O9 and symmetry equivalents) μ-bridging to the central $\{Gd_4\}$ square. The Mn ions lie in distorted octahedral geometries in $\{O_6\}$ coordination spheres with the Jahn-Teller axes (O10-Mn2, 2,225 Å, Mn2-O16, 2.218 Å; O5-Mn4, 2.261 Å, Mn4-O12, 2.221 Å) described by the DMF-Mn-OH vectors; *i.e.* across the diagonal of the $\{Mn_4\}$ square. The Gd(III) ions are eight coordinate and are in distorted square antiprismatic geometries with their remaining coordination sites filled by a combination of terminal H_2O molecules, which form intra-

molecular H-bonds to the terminally bonded O-atoms of the C4 ligands (e.g. O8…O11, 2.642 Å) and inter-molecular H-bonds to hydroxide anions, and DMF molecules.

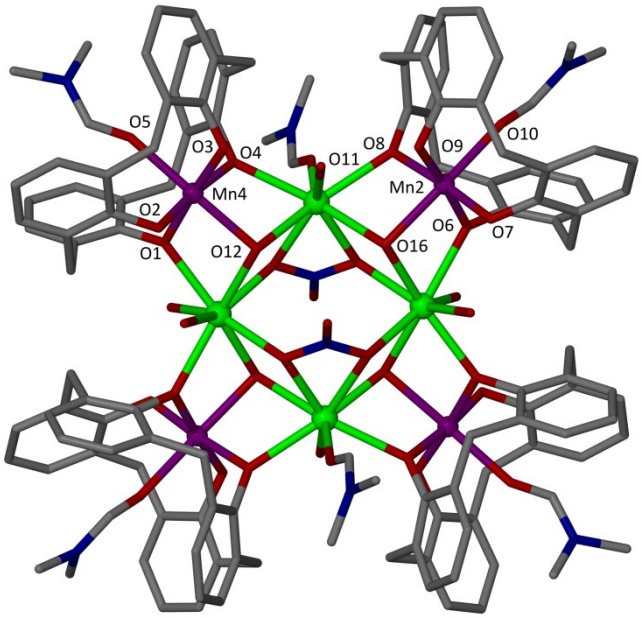

Figure 2. Molecular structure of **1** showing the coordination environments around the Mn^{III} and Gd^{III} centres. Hydrogen atoms, hydroxide anions and co-crystallized DMF molecules omitted for clarity. Colour code as in Figure 1; Ln = green.

Examination of the extended structures of **1** – **3** shows that symmetry equivalent clusters pack together to form two types of complex arrangement. Disorder is present in the solvent molecules co-crystallised with the clusters in each of the crystal lattices, and this is severe enough to preclude detailed analysis of the inter-molecular interactions between all of the structural components in each crystal structure. The structure of **1** differs to those of **2** and **3** (isostructural), and packing of the asymmetric unit shows that four [Mn(III)-C4] sub-units assemble in a pseudo-capsule assembly to produce a DMF rich microenvironment between the corner units of nearest-neighbour clusters (Figure 3A). These are reminiscent of hexameric calixarene based molecular capsules, and suggest that appropriately functionalized C4 molecules could be employed in cluster formation to invoke templated self-assembly into nanometer scale assemblies containing large internal volumes.[16a,c,e] The extended structures of isostructural **2** and **3** (Figure 3B) show the formation of a similar type of pseudo-capsule assembly. Three [Mn(III)-C4] sub-units assemble to produce a second type of DMF microenvironment, while the fourth neighbouring sub-unit points away from the centre of the capsule-like assembly. Notably, the [Mn(III)-C4] sub-unit found in the $[Mn^{III}_2Mn^{II}_2]$ SMM shown in Figure 1B is preserved in these new hybrid 3*d*-4*f* complexes. This indicates that this is indeed a favourable structural sub-unit (or "metalloligand") for Mn(III), and that these moieties may well be exploited in

the formation of other complexes and supramolecular architectures, whose self-assembly may be governed by relatively small changes in reaction conditions.

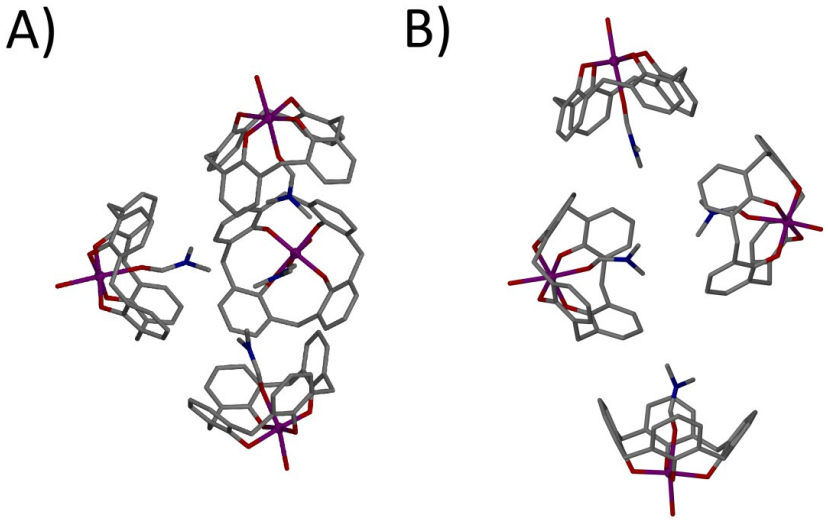

Figure 3. Partial extended structures of **1**(A) and **2**(and isostructural **3**, B) showing the packing of [Mn(III)-C4] sub-units in each case. A) Four corner units of nearest-neighbour clusters form a pseudo-capsule assembly containing a DMF microenvironment that is reminiscent of other calixarene based molecular capsules.[16a,c,e] B) Three corner units of nearest-neighbour clusters form a related assembly, albeit with one pointing away from the DMF microenvironment relative to that shown in A. Figures not to scale.

Magnetic Studies

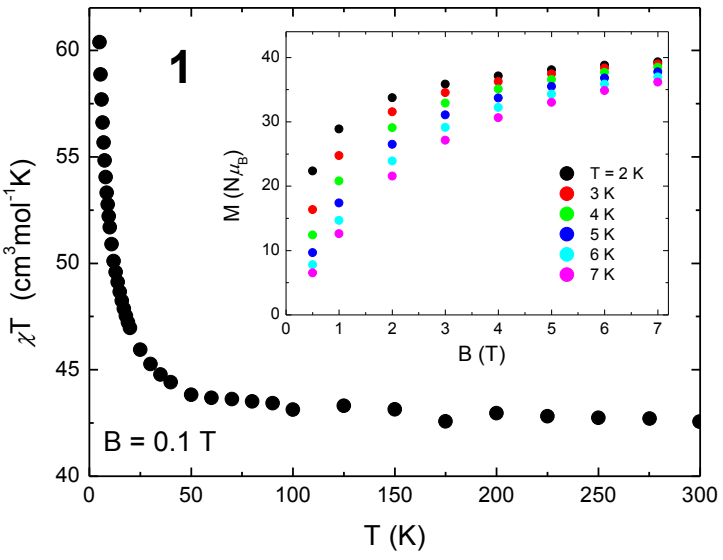

← ***Figure 4.*** Temperature dependence (5 – 300 K) of the dc-susceptibility for **1** collected in an applied field of 0.1 T. Inset: magnetisation of **1** versus applied field for several temperatures.

We investigated the magnetic properties of **1** by dc-susceptibility experiments in the 300 – 5 K temperature range in an applied field B of 0.1 T (Figure 4). The room-temperature χT value of ~42.8 cm^3 K mol^{-1} is close to the spin-only ($g = 2.0$) value expected for an uncoupled $[Mn^{III}_4Gd^{III}_4]$ unit of ~43.5 cm^3 K mol^{-1}. The value stays essentially constant as the temperature is decreased until approximately 50 K, below which it increases, reaching a maximum of ~60.5 cm^3 K mol^{-1} at 5 K. This behaviour is suggestive of very weak intra-molecular exchange and one would expect a nesting, and thus population of, several S states even at the lowest temperatures studied. This is reflected in the low temperature χT value, which is well below that expected for a ferromagnetically coupled cluster with an isolated $S = 22$ ground state (253 cm^3 K mol^{-1}), and can also be seen in the magnetisation versus field data (collected in the 2 – 7 K temperature range for applied fields up to 7 T, and plotted in the inset of Figure 4) which shows M increasing only slowly with B, rather than quickly reaching saturation as one would expect for an isolated spin ground state. This is indicative of the population of low lying levels with smaller magnetic moment, which only become depopulated with the application of a large field. This result suggests **1** to be an excellent candidate for magnetic refrigeration.[15b] To validate this statement, our preliminary studies focused on the determination of the magnetic entropy change ΔS_m of **1** by analysing the experimental $M(B)$ data of Figure 4. In an isothermal process of magnetisation, ΔS_m can be derived from the Maxwell relations by integrating over the magnetic field change $\Delta B = B_f - B_i$, i.e., $\Delta S_m(T)_{\Delta B} = \int[\partial M(T,B)/\partial T]_B dB$.[1,2,5] The so-obtained ΔS_m is depicted in Figure 5 for several field changes. It can be seen that $-\Delta S_m$ increases gradually with increasing ΔB reaching a value of 19.0 J kg^{-1} K^{-1} at $T = 4$ K, achieved for the experimentally accessible maximum ΔB of 7 T. This is amongst the highest values ever reported for this temperature range.[5] We also note that the observed magnetic entropy changes are much larger than the maximum allowable entropy for an isolated $S = 22$ spin ground state, i.e. $R \ln(2S + 1) = 3.8\ R = 9.0$ J kg^{-1} K^{-1}. This demonstrates that the presence of low-lying excited spin states can have a strong and positive influence on the magneto-caloric effect.[5]

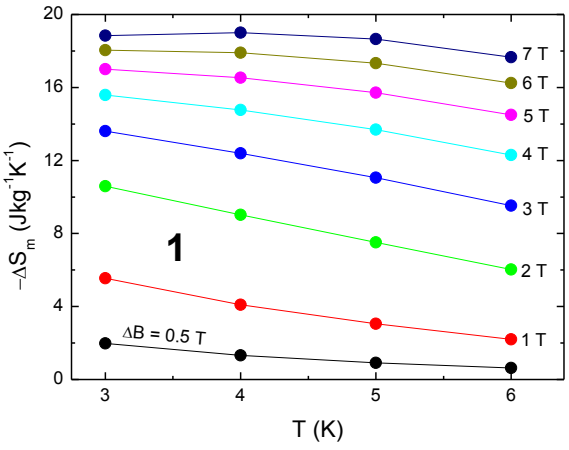

Figure 5. Temperature dependencies of the magnetic entropy change of **1** for applied field changes ΔB.

We next turn to the study of the magneto-caloric effect of **1** by means of heat capacity (C) experiments, emphasizing that the measurement of the heat capacity as a function of temperature in constant magnetic field provides the most complete characterisation of the MCE in magnetic materials.[2,5] The top panel of Figure 6 depicts the experimental heat capacity curves of **1** in the 30 – 0.3 K temperature range for several applied fields. It can be seen that the curves collected at temperatures below 1 K are strongly dependent on the applied field, and that they span over three orders of magnitude in units of R for the investigated field changes. The zero-field curve achieves a maximum of ~4 R for T = 0.8 K, whilst the field-independent lattice contribution has a value of 6×10^{-3} R for the same temperature. The relevant feature is the broad specific heat anomaly that shifts towards higher temperatures on increasing applied field; we attribute this to the field-splitting of the spin multiplets of the molecule. We stress, however, that this behaviour cannot be reproduced by a simple model based on a well-defined S = 22 spin ground state (which would not exceed ~1 R). To explain the excess of experimental heat capacity, we need to invoke the contribution arising from the population of low-lying excited spin states, corroborating the previous magnetisation experiments. In the high-temperature range a large field-independent contribution appears that can be attributed to the lattice phonon modes of the crystal. The dashed line in the top panel of Figure 6 represents a fit to this contribution with the well-known low-temperature Debye function, yielding a value of Θ_D = 23 K for the Debye temperature, typical for this class of cluster complex.[1b]

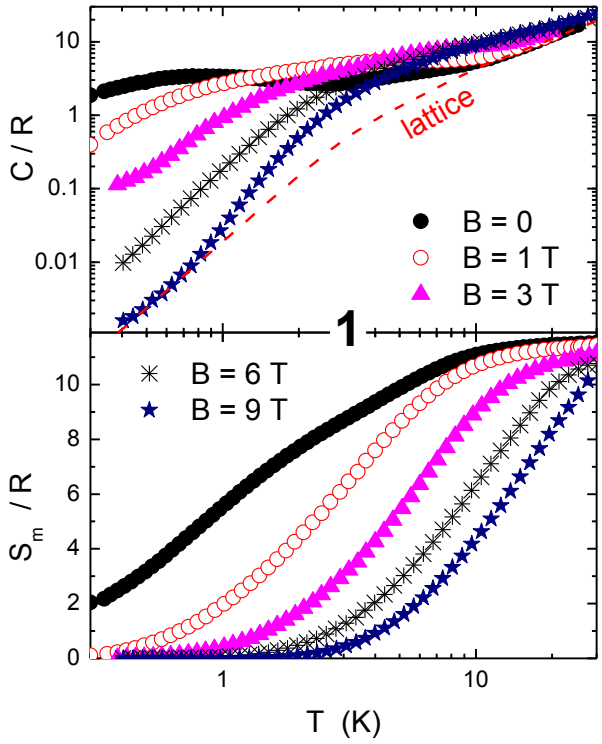

← ***Figure 6.*** Top: temperature dependencies of the heat capacity of **1** normalised to the gas constant R collected for B = 0, 1, 3, 6 and 9 T. Dashed line is the fitted lattice contribution. Bottom: temperature dependencies of the experimental magnetic entropy for several B, as obtained from the respective magnetic contributions to the total heat capacity.

From the experimental heat capacity, the temperature dependence of the magnetic entropy S_m is obtained by integration, i.e., using $S_m(T,B) = \int C_m/T \, dT$, where the magnetic heat capacity C_m is obtained from C upon subtracting the lattice contribution. The so-obtained S_m is shown in the bottom panel of Figure 6 for the corresponding applied fields. As further evidence of the participation of excited spin states, we note that the experimental $S_m(T)$ by far exceeds the value expected for an isolated $S = 22$ ground state, i.e. 3.8 R.

It now becomes straightforward to obtain the magnetic entropy changes ΔS_m of **1**, whose temperature-dependencies are depicted in the top panel of Figure 7 for several field changes. Any uncertainty in the determination of the field-independent lattice contribution is irrelevant for this calculation and cancels out since we are dealing with differences between entropies. The $\Delta S_m(T,\Delta B)$ curves are consistent with the preliminary estimates obtained in Figure 5, proving the validity of employing both the magnetization and heat capacity data in the analysis. Furthermore, we observe that $-\Delta S_m$ reaches the extremely very large value of 21.3 J kg^{-1} K^{-1} at liquid-helium temperature for the investigated field change $\Delta B = (9 - 0)$ T.

The analysis of the heat capacity data also permits us to estimate the adiabatic temperature change ΔT_{ad} by using $\Delta T_{ad}(T)_{\Delta B} = [T(S_m)_{Bf} - T(S_m)_{Bi}]S_m$ directly from the experimental magnetic entropy S_m depicted in Figure 6 (bottom panel). The bottom panel of Figure 7 shows that the maximum in ΔT_{ad} gradually decreases and shifts to lower temperatures by decreasing the field change ΔB. Indeed, it changes from $\Delta T_{ad} = 9.0$ K for $\Delta B = (9 - 0)$ T at $T = 4.4$ K to $\Delta T_{ad} = 2.0$ K for $\Delta B = (1 - 0)$ T at $T = 2.0$ K. In other words the magnetic field dependence of the adiabatic temperature change increases from 1 to 2 K/T, respectively, making **1** one of the finest refrigerants in the liquid-helium temperature range.[2,15b]

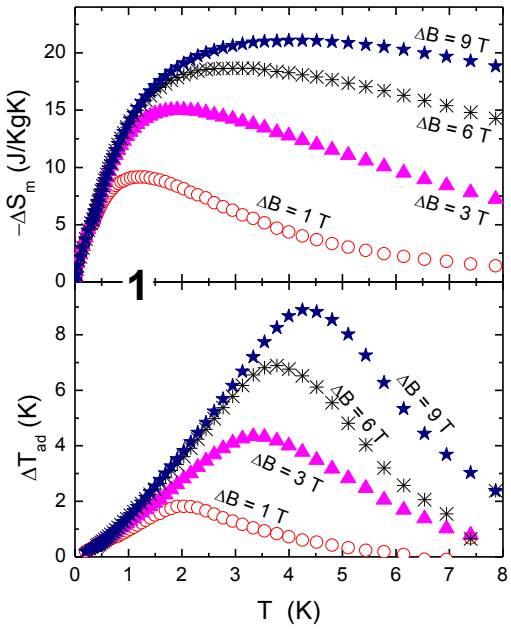

Figure 7. → Top: temperature dependencies of the magnetic entropy change of **1** for the indicated applied-field changes ΔB. Bottom: temperature dependencies of the adiabatic temperature change of **1** for the indicated ΔB. Both $\Delta S_m(T,\Delta B)$ and $\Delta T_{ad}(T,\Delta B)$ curves are obtained from the heat capacity data of Figure 6.

We have stressed throughout the text that negligible anisotropy is a major requirement for achieving an enhanced magneto-caloric effect with polymetallic molecules. As is well established, a large magnetic anisotropy promotes single-molecule magnet (SMM) behaviour, for which slow relaxation of the net spin per molecule is obtained below a super-paramagnetic blocking temperature. The consequence is that the blocked molecular spins tend to lose thermal contact with the lattice at low temperatures,[25] resulting in a lower magnetic entropy and therefore a lower MCE. The effect of the anisotropy on the efficiency of a polymetallic molecule in terms of magnetic refrigeration has already been demonstrated by means of simple numerical simulations, and experimentally using a large variety of molecules from the prototype Mn_{12} SMM to the [ideally] isotropic Mn_{10} supertetrahedron.[5] However, to the best of our knowledge, no example has yet been provided of a molecular refrigerant in which the degree of anisotropy can be experimentally and exclusively altered/tuned without structural alteration. The $[Mn^{III}_4Ln^{III}_4]$ molecular cluster can provide such a playground since the identity of the Ln(III) can be easily changed. By replacing the zero-orbital moment Gd^{III} ion (**1**) with the anisotropic Tb^{III} (**2**) or Dy^{III} (**3**) ion, one can expect to observe abrupt changes in the magneto-thermal properties of these otherwise structurally analogous molecules.

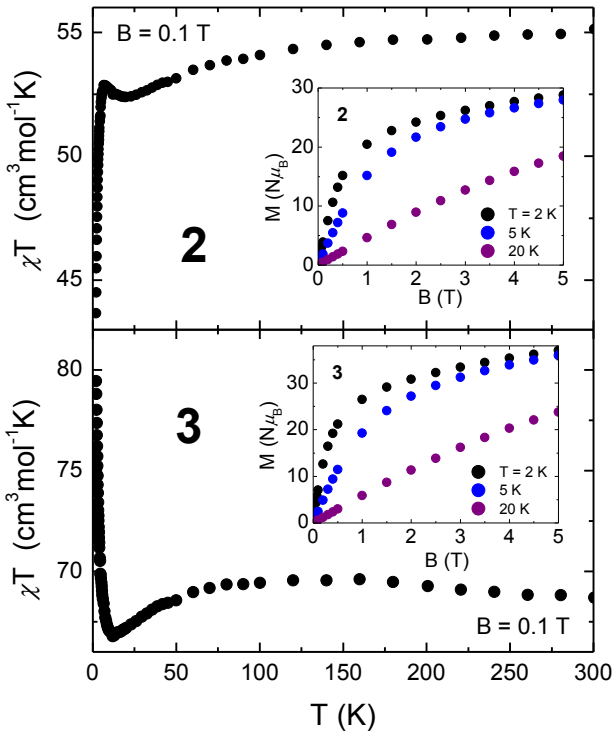

Figure 8. Temperature dependence (5 – 300 K) of the dc-susceptibility for **2** (top) and **3** (bottom) collected in an applied field of 0.1 T. Insets: magnetisation of **2** (top) and **3** (bottom) versus applied field for T = 2, 5 and 20 K.

Figure 8 depicts the dc-susceptibility measurements for **2** and **3**, collected in the 300 – 2 K temperature range for an applied field B of 0.1 T. Let us first examine complex **2**; terbium(III) is a non-Kramers ion with a $^7F_6$ ground state. The fit of the experimental $\chi(T)$ data to the Curie-Weiss law in the 300 – 5 K temperature range provides a small $\theta = -0.16$ K, suggesting that the metallic ions are only weakly magnetically correlated. The room-temperature χT value of **2** is ~55.5 cm^3 K mol^{-1} in reasonable agreement with the spin-only ($g = 2.0$) value expected for an uncoupled $[Mn^{III}_4Tb^{III}_4]$ unit of ~59.3 cm^3 K mol^{-1}. The value stays essentially constant as the temperature is decreased until approximately 150 K, below which it decreases smoothly down to 22 K reaching a value of ~52.3 cm^3 K mol^{-1}. The 22 – 7 K temperature range is marked by an upward shift in the χT value that, considering the relatively large inter-cluster spacing, we associate to ferro- or ferrimagnetic intra-molecular exchange. In the lowest temperature range, χT sharply decreases to ~43.5 cm^3 K mol^{-1} at 2 K, suggesting either antiferromagnetism or perhaps more likely the progressive depopulation of excited states of the lanthanide ions. A similar conclusion may be drawn by looking at the field dependence of the magnetisation (inset of Figure 8, top panel). On increasing field, the onset of a net molecular moment promotes a relatively quick increase of the magnetisation reaching 20.5 $N\mu_B$ at B = 1 T for $T = 2$ K, after which it increases linearly without saturating. Likewise for **3**, we expect the crystal field to split the $^6H_{15/2}$ ground state of dysprosium(III). Contrary to **2**, the fit of the experimental $\chi(T)$ data to a Curie-Weiss law in the 300 – 5 K temperature range provides a very small, but positive value [$\theta = +0.35$ K] suggesting that the ferro- or ferrimagnetic component is relatively stronger in **3**. The $\chi T(T)$ value stays essentially constant from room temperature down to nearly 100 K, below which it experiences a small decrease to ~66.8 cm^3 K mol^{-1} at $T = 12.6$ K. The lowest temperature range is then characterised by an abrupt increase in χT, which reaches ~79.5 cm^3 K mol^{-1} at $T = 2$ K, corroborating the presence of a stronger ferro- or ferrimagnetic interaction than observed in **2**. This is also supported by the larger experimental values of the magnetisation, whose field dependence [qualitatively] is very similar to that of **2** (inset of Figure 8, bottom panel).

Because of the anisotropy induced by the Tb^{III} and Dy^{III} ions, and the observation that each molecular unit develops a net magnetic moment at low temperatures, it is reasonable to expect super-paramagnetic behaviour. We therefore investigated the dynamic properties of **2** and **3** by means of ac-susceptibility experiments. Both complexes show out-of-phase signals (χ'') at temperatures above 2 K (Figure S1), indicative of either a phase transition or slow relaxation of the magnetisation. In order to discriminate between these two phenomena, we extended our experiments to the lower temperature region, obtaining the results depicted in Figure 9.

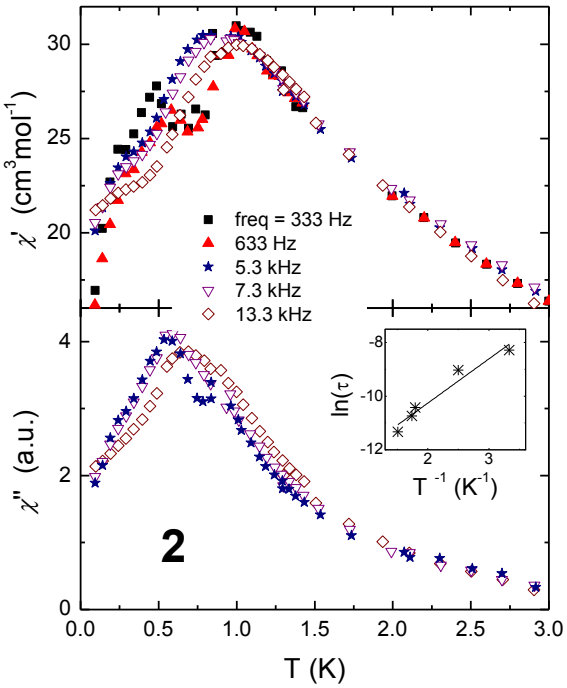

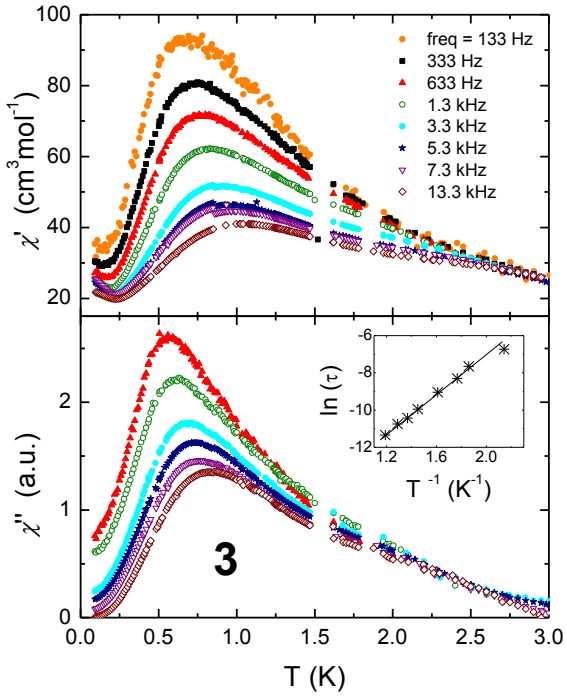

Figure 9. Temperature dependence of the in-phase (χ', top) and out-of-phase (χ'', bottom) ac-susceptibility for **2** (left) and **3** (right), collected in zero-applied field and for the indicated excitation frequencies. Insets: semi-logarithmic plots of the (main) zero-field relaxation time. The straight lines are fits to the Arrhenius law.

The main feature is a cusp in the in-phase component χ' of the ac-susceptibility which occurs at approximately 0.9 K for both complexes, accompanied by a non-zero out-of-phase component (Figure 9), with both maxima in χ' and χ'' being frequency (f) dependent. The experimental data suggest super-paramagnetic blocking of the molecular spins below T_B corresponding to the temperature at maximum absorption. Using the average value T_B = 0.9 K, the frequency shift of T_B, nominally $\Delta T_B/(T_B \Delta \log f)$, where ΔT_B is the change in T_B for the given change in frequency $\Delta \log f$, provides the values of 0.5 and 0.2 for **2** and **3**, respectively, which are comparable to that of other super-paramagnets.[26] The relaxation time for superparamagnets with an anisotropy barrier U is usually described with the Arrhenius law, typical of a thermal activation process: $\tau = \tau_0 \exp(U/k_BT)$, where $\tau = 1/2\pi f$ and τ_0 is an attempt frequency. We have fitted the cusp in the out-of-phase susceptibility with the above equation. The results are presented in Figure 9 (insets), affording $\tau_0 = 1\times10^{-7}$ s and U/k_B = 3.0 K for **2**, and $\tau_0 = 3\times10^{-8}$ s and U/k_B = 5.0 K for **3**. Closer inspection of the low-temperature ac-susceptibility (Figure 9) reveals that the magnetic relaxation in these materials is particularly complex, since other (secondary) relaxation pathways can be spotted besides the main one taking place at 0.9 K. Indeed, for both complexes, a rather broad frequency-dependent "shoulder" is observed in the 2 – 3 K temperature range. For **2**, a secondary cusp is observed in $\chi''(T)$ at somewhat higher temperature than that of the main feature. For **3**, the maximum absorption of a faster relaxation mechanism takes place below 80 mK, temperatures not experimentally accessible with our setup.

The frequency dependence of the ac-susceptibility below 3 K suggests that both **2** and **3** are single-molecule magnets. Therefore, it is not a surprise that heat capacity experiments performed on **2** and **3** (Figure 10) can detect no sign of long-range magnetic order (in the form of a sharp lambda-like anomaly), a result also expected on the basis of structure considerations (see above). The complicated magnetic behaviour of these materials is also observed in Figure 10. For example the zero-field C curve of complex **2** shows a broad anomaly close to T = 3 K, followed by a second one at 1 K, and a third detected at the lowest investigated temperature, the latter being clearly visible in case of in-field measurements.

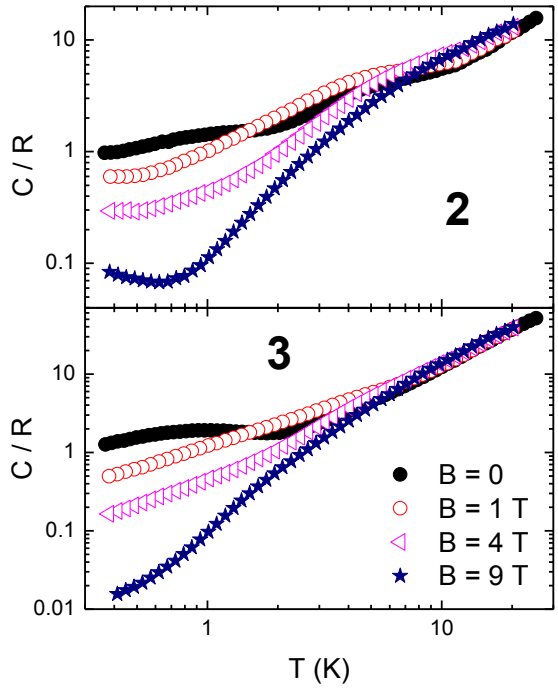

Figure 10. Temperature dependence of the heat capacity normalised to the gas constant *R* for **2** (top) and **3** (bottom) collected for B = 0, 1, 4 and 9 T, as labeled.

The measurements of the heat capacity of **2** and **3** indicate that these molecules would not be suitable for use as molecular refrigerants. This is simply understood by looking at the field-dependent curves and their absolute values in units of *R*. By comparing the results of Figure 10 with that obtained with an excellent refrigerant such as **1** (Figure 6), it can be seen that the zero-field heat capacities of **2** and **3** are notably smaller than that of **1** in the (magnetic dependent) low-temperature region. Furthermore, the change of applied field from 0 to 9 T causes the heat capacities of **2** and **3** to change by one-to-two orders of magnitude at best, i.e. more than an order of magnitude less than in **1**. Likewise, the changes in the magnetic entropy follow the same trend, allowing us to conclude that the anisotropy of the lanthanide ion is of crucial importance for dictating the performance of this family of molecules as magnetic refrigerants.

Conclusions

To conclude, we have expanded our initial studies into $[Mn^{III}_4Ln^{III}_4]$ cluster formation with calixarenes as supporting ligands so that we tailor these 3*d*/4*f* clusters of general formula

$[Mn^{III}_4Ln^{III}_4(OH)_4(C4)_4(NO_3)_2(DMF)_6(H_2O)_6](OH)_2$ to include either Gd, Tb or Dy as desired. Magnetic studies show that the $[Mn^{III}_4Gd^{III}_4]$ cluster is an excellent magnetic refrigerant for low-temperature applications. The molecular anisotropy added by replacing Gd with Tb or Dy results in (a) superparamagnetic behaviour of the $[Mn^{III}_4Tb^{III}_4]$ and $[Mn^{III}_4Dy^{III}_4]$ clusters with blocking temperatures in the temperature region below 1 K, and (b) poor performance of these clusters in terms of magnetic refrigeration. The [Mn(III)-C4] sub-unit is common to $[Mn^{III}_2Mn^{II}_2]$ SMMs and the $[Mn^{III}_4Ln^{III}_4]$ clusters reported here, and we are currently exploring the use of this moiety in the formation of alternative cluster assemblies through variation in reaction conditions. The substitution of other lanthanides in the $[Mn^{III}_4Ln^{III}_4]$ cluster motif is underway with a view to fully characterising the magnetic properties of the entire series of analogous clusters.

References

[1] (a) Spichkin, Yu. I.; Zvezdin, A. K.; Gubin, S. P.; Mischenko, A. S; Tishin, A. M. *J. Phys. D: Appl. Phys*., **2001**, *34*, 1162. (b) Evangelisti, M.; Luis, F.; de Jongh, L. J.; Affronte, M. *J. Mater. Chem*., **2006**, *16*, 2534.

[2] See for example: (a) Zimm, C.; Jastrab, A.; Sternberg, A.; Pecharsky, V. K.; Gschneidner Jr., K. A.; Osborne, M.; Anderson, I. *Adv. Cryog. Eng*., **1998**, *43*, 1759; (b) Pecharsky, V. K.; Gschneidner Jr., K. A. *J. Magn. Magn. Mater*., **1999**, *200*, 44; (c) Gschneidner Jr., K. A.; Pecharsky, A. O.; Pecharsky, V. K. in *CryocoolersII*, ed. R. S. Ross Jr., Kluwer Academic/Plenum Press, New York, **2001**, p. 433.

[3] (a) Debye, P. *Ann. Phys*., **1926**, *81*, 1154; (b) Giauque, W. F. *J. Am. Chem. Soc*., **1927**, *49*, 1864.

[4] Feder, T. *Physics Today,* **2009**, *62*, 21.

[5] Evangelisti, M.; Brechin E, K.; *Dalton Trans*., **2010**, *39*, 4672, and references therein.

[6] (a) Torres, F.; Hernández, J. M.; Bohigas, X.; Tejada, J. *Appl. Phys. Lett*., **2000**, *77*, 3248. (b) Torres, F.; Bohigas, X.; Hernández, J. M.; Tejada, J. *J. Phys.: Condens. Matter*, **2003**, *15*, L119.

[7] Zhang, X. X.; Wei, H. L.; Zhang, Z. Q.; Zhang, L. *Phys. Rev. Lett*., **2001**, *87*, 157203.

[8] Affronte, M.; Ghirri, A.; Carretta, S.; Amoretti, G.; Piligkos, S.; Timco, G. A.; Winpenny, R.E. P. *Appl. Phys. Lett*., **2004**, *84*, 3468.

[9] (a) Evangelisti, M.; Candini, A.; Ghirri, A.; Affronte, M.; Brechin, E. K.; McInnes, E. J. L.; *Appl. Phys. Lett*., **2005**, *87*, 072504. (b) Low, D. M.; Jones, L. F.; Bell, A.; Brechin, E. K.; Mallah, T.; Rivière, E.; Teat, S. J.; McInnes, E. J. L. *Angew. Chem. Int. Ed*., **2003**, *42*, 3781. (c) Shaw, R.; Laye, R. H.; Jones, L. F.; Low, D. M.; Talbot-Eeckelaers, C.; Wei, Q.; Milios, C. J.; Teat, S. J.; Helliwell, M.; Raftery, J.; Evangelisti, M.; Affronte, M.; Collison, D.; Brechin, E. K.; McInnes, E. J. L. *Inorg. Chem*., **2007**, *46*, 4968.

[10] Manoli, M.; Johnstone, R. D. L.; Parsons, S.; Murrie, M.; Affronte, M.; Evangelisti M.; Brechin, E. K. *Angew. Chem. Int. Ed*., **2007**, *46*, 4456.

[11] Manoli, M.; Collins, A.; Parsons, S.; Candini, A.; Evangelisti, M.; Brechin, E. K. *J. Am. Chem. Soc*., **2008**, *130*, 11129.

[12] Ma, S.; Cui, W. B.; Li, D.; Sun, N. K.; Geng, D. Y.; Jiang, X.; Zhang, Z. D. *Appl. Phys. Lett*., **2008**, *92*, 173113.

[13] Brechin, E. K. *Chem. Commun*., **2005**, 5141.

[14] (a) Brechin, E. K.; Soler, M.; Davidson, J.; Hendrickson, D. N.; Parsons, S.; Christou, G. *Chem. Commun*., **2002**, 2252. (b) Piligkos, S.; Rajaraman, G.; Soler, M.; Kirchner, N.; van Slageren, J.; Bircher, R.; Parsons, S.; Güdel, H.-U.; Kortus, J.; Wernsdorfer, W.; Christou, G.;. Brechin, E. K. *J. Am. Chem. Soc*., **2005**, *127*, 5572.

[15] (a) Scott, R. T. W.; Parsons, S.; Murugesu, M.; Wernsdorfer, W.; Christou, G.; Brechin, E. K. *Angew. Chem. Int. Ed*., **2005**, *44*, 6540. (b) Evangelisti, M.; Candini, A.; Affronte, M.; Pasca, E.; de Jongh, L. J.; Scott, R. T. W.; Brechin, E. K. *Phys. Rev. B*, **2009**, *79*, 104414.

[16] For example see: (a) MacGillivray, L. R.; Atwood, J. L. *Nature*, **1997**, *389*, 469. (b) Orr, G. W.; Barbour, L. J.; Atwood, J. L. *Science*, **1999**, *285*, 1049. (c) Gerkensmeier, T.; Iwanek, W.; Agena, C.; Froehlich, R.; Kotila, S.; Nather, C.; Mattay, J. *Eur. J. Org. Chem*. **1999**, 2257. (d) Atwood, J. L.; Barbour, L. J.; Dalgarno, S. J.; Hardie, M. J.; Raston, C. L.; Webb, H. R. *J. Am. Chem. Soc.*, **2004**, *126*, 13170. (e) Dalgarno, S. J.; Tucker, S. A.; Bassil, D. B.; Atwood, J. L. *Science*, **2005**, *309*, 2037. (f) Ugono, O.; Holman, K. T. *Chem. Commun*., **2006**, 2144. (g) Barrett, E. S.; Dale, T. J.; Rebek Jr., J. *J. Am. Chem. Soc*. **2007**, *129*, 3818.

[17] Gutsche, C. D. *Acc. Chem. Res.*, **1983**, *16*, 161.

[18] Gutsche, C. D. *Calixarenes 2001*, Kluwer Academic Publishers, **2001**, Chapter 1 and references therein.

[19] See for example: (a) Petrella, A. J.; Raston, C. L. *J. Organomet. Chem.*, **2004**, *689*, 4125. (b) Homden, D. M.; Redshaw, C. *Chem. Rev.*, **2008**, *108*, 5086. (c) Aronica, C.; Chastanet, G.; Zueva, E.; Borshch, S. A.; Clemente-Juan, J. M.; Luneau, D. *J. Am. Chem. Soc.* **2008**, *130*, 2365.

[20] (a) Karotsis, G.; Teat, S. J.; Wernsdorfer, W.; Piligkos, S.; Dalgarno, S. J.; Brechin, E. K. *Angew. Chem. Int. Ed*., **2009**, *48*, 8285. (b) Karotsis, G.; Kennedy, S.; Dalgarno, S. J.; Brechin, E. K. *Chem. Commun*., **2010**, 46, 3884. (c) Karotsis, G.; Evangelisti, M.; Dalgarno, S. J.; Brechin, E. K. *Angew. Chem. Int. Ed*., **2009**, *48*, 9928.

[21] Aronica, C.; Chastanet, G.; Zueva, E.; Borshch, S. A.; Clemente-Juan J. M.; Luneau, D. *J. Am. Chem. Soc.* **2008**, *130*, 2365.

[22] (a) Desroches, C.; Pilet, G.; Borshch, S. A.; Parola, S.; Luneau, D. *Inorg. Chem.* **2005**, *44*, 9112. (b) Desroches, C.; Pilet, G.; Szilágyi, P. A.; Molnár, G.; Borshch, S. A.; Bousseksou, A.; Parola, S.; Luneau, D. *Eur. J. Inorg. Chem.* **2006**, 357. (c) Kajiwara, T.; Iki, N.; Yamashita, M. *Coord. Chem. Rev.*, **2007**, *251*, 1734. (d) Bi, Y.; Wang, X.-T.; Liao, W.; Wang, X.; Wang, X.; Zhang, H.; Gao, S. *J. Am. Chem. Soc.*, **2009**, *131*, 11650. (e) Bilyk, A.; Dunlop, J. W.; Fuller, R. O.; Hall, A. K.; Harrowfield, J. M.; Wais Hosseini, M.; Koutsantonis, G. A.; Murray, I. W.; Skelton,

B. W.; Stamps, R. L.; White, A. H. *Eur. J. Inorg. Chem.*, 2010, 2106. (f) Bilyk, A.; Dunlop, Hall, A. K.; Harrowfield, J. M.; Wais Hosseini, M.; Koutsantonis, Skelton, B. W.; White, A. H. *Eur. J. Inorg. Chem.*, 2010, 2089; (g) Bilyk, A.; Dunlop, J. W.; Fuller, R. O.; Hall, A. K.; Harrowfield, J. M.; Wais Hosseini, M.; Koutsantonis, G. A.; Murray, I. W.; Skelton, B. W.; Sobolev, A. N.; Stamps, R. L.; White, A. H. *Eur. J. Inorg. Chem.*, 2010, 2127.

[23] Spek, A. L. *Acta Cryst. A46* 1990, C34.

[24] Mereacre, V.; Ako, A.; M.; Filoti, G.; Bartolomé, J.; Anson, C. E.; Powell, A. K. *Polyhedron*, **2010**, 29, 244.

[25] Evangelisti, M.; Luis, F.; Mettes, F. L.; Aliaga, N.; Aromí, G.; Alonso, J. J.; Christou, G.; de Jongh, L. J. *Phys. Rev. Lett.* **2004**, *93*, 117202.

[26] Mydosh, J. A. in "Spin glasses: an experimental introduction", Taylor and Francis, London, 1993.